Title
Mixing in the dome region of a staged gas turbine combustor

Journal
Journal of Propulsion and Power, 9(5)

ISSN
0748-4658

Authors
Sowa, WA
Brady, RA
Samuelsen, GS

Publication Date
1993-09-01

DOI
10.2514/3.23678

JOURNAL OF PROPULSION AND POWER
Vol. 9, No. 5, Sept.–Oct. 1993

Mixing in the Dome Region of a Staged Gas Turbine Combustor

W. A. Sowa,* R. A. Brady,† and G. S. Samuelsen‡
University of California, Irvine, Irvine, California 92717

Many modifications to the combustion process are being proposed and evaluated to lower NO_x emissions from gas turbine engines in both stationary and propulsion applications. A promising technique is staged combustion, wherein the fuel is mixed into a fuel-rich region and the final air is injected downstream to an overall lean mixture. This article examines the effect of dome design and operational changes on the mixing quality in the fuel-rich region. A statistical analysis is employed to establish the parametric sensitivity in this complex flow. A mixing effectiveness index is defined and used to optimize the gas species uniformity and the extent of reaction at the exit plane of the dome. The results reveal that mixing effectiveness is intimately tied to the fuel and air injection locations, the macroscale structure of the dome aerodynamics, and the level of turbulence. Increases in nozzle/air to fuel ratio, reference velocities, and the dome expansion angle increased the level of turbulence. The optimum configuration featured counterswirling fuel and airstreams and produced a strong torroidal recirculation zone, an effective spray angle of 45 deg, and azimuthal velocities that decayed to zero inside of two duct diameters. Due to the intimate relationship between variables, the response of mixing to changes in any single variable cannot be considered independently of the other variables. The results underscore the system specific nature of mixing optimization.

Introduction

MIXING quality has been recognized as an important key to obtaining low NO_x combustor performance goals in gas-fired[1–4] and liquid-fired[5–7] combustion systems. Mixing strategies vary widely depending on the type of fuel used and the application. The focus of this article is on the mixing quality in the dome region of liquid-fired staged combustors, and the sensitivity of mixing to the inlet boundary and operating conditions.

The application of staged combustion to liquid-fired gas turbines to reduce NO_x emissions was introduced in the 1970s.[8] After a decade of relative inactivity, studies have recently been initiated to identify effective mixing approaches in both the fuel-rich and air addition stages of these combustors.[7,9] This research is especially important given the trend to produce more efficient and lighter gas turbine engines by increasing the operating temperatures and pressures in the combustors.

The dome region of the staged liquid-fired combustor differs from the conventional combustor in two important ways. First, the dome region of the staged combustor has no primary air inlet holes. Because of this, closure of the recirculation zone is accomplished by the contraction provided at the entrance to the quick mixing zone. In addition, the rich zone of the staged combustor cannot rely on transpiration cooling of its liner since the additional air causes localized stoichiometric packets of fuel and air to be created.

In a staged gas turbine combustor, effective mixing of the independently injected fuel and air is critical. Ineffective mixing in the dome will lead to increased residence times of stoichiometric and near-stoichiometric packets of fuel and air which can promote the formation of NO_x.[10] Nonuniform gas temperatures and gas species profiles can also degrade the performance of the air addition stage. In addition, ineffective mixing can result in higher than necessary rms fluctuations of temperature and species concentration which can correlate with degraded performance. Effective mixing, on the other hand, "marries" the atomization and evaporation processes with the air to provide optimum dome performance.

Several elements in the dome design effect mixing quality, including fuel atomization quality,[6,11] fuel injection location,[2–4,12,13] swirl,[1,7,14] and dome chamber dimensions.[15–17]

The wealth of previous work represents a significant foundation for interpretation of results and guidance. However, the dependence of specific results on the experimental constraints of fuel type, firing mode, and geometry is graphically illustrated in comparing conclusions between Charles and Samuelsen[16] and Cameron et al.[15] Using a model gas turbine combustor without sidewall air addition and fueled by propane, Charles[16] noted an improvement in fuel-air mixing when a step expansion between the outer swirl hub and the wall cooling air passage was changed to a 45-deg expansion. Cameron,[15] on the other hand, found no dramatic changes in flowfield structure as the dome geometry was varied from a step to a 45-deg expansion in a liquid-fired model gas turbine combustor with side wall air addition. The contrasting results of these two studies highlights the need to carefully consider the interrelationship of design and operational variables when interpreting system performance.

While studies have been conducted to understand how design and operational constraints correlate with mixing performance in flames, the work is specific to select fuels, firing modes, and geometries that are different from the dome of a liquid-fired staged combustor except in general terms. This article focuses on the experimental evaluation of mixing quality, and the correlation of mixing quality with design and operational characteristics of the dome section in a liquid-fired staged combustor.

Experimental Facility

A cylindrical staged combustor dome (80-mm diameter) was used to model the geometry of a practical staged can combustor as shown in Fig. 1. Like other laboratory model

Presented as Paper 92-3089 at the AIAA 28th Joint Propulsion Conference, Nashville, TN, July 6–8, 1992; received July 28, 1992; revision received April 12, 1993; accepted for publication April 17, 1993.

*Associate Director, UCI Combustion Laboratory. Member AIAA.
†Graduate Researcher, UCI Combustion Laboratory. Student Member AIAA.
‡Professor, Director, UCI Combustion Laboratory. Associate Fellow AIAA.

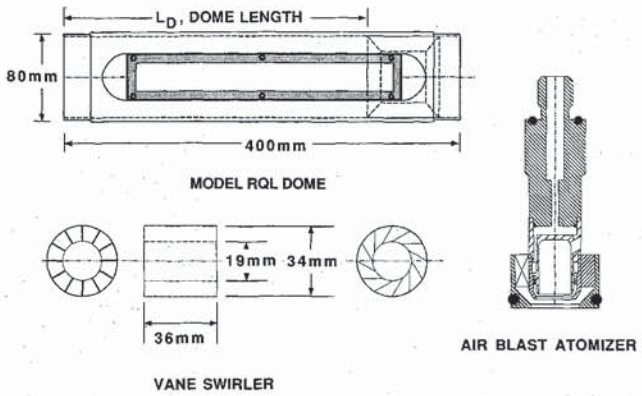

Fig. 1 Experimental stage combustor dome, swirler, and atomizer. The distance L_D represents the distance from the atomizer to the combustor convergence.

combustors described by Brouwer et al.[18] and Cameron,[15] this combustor featured a stainless steel shell with optical access and a variable geometry inlet plane. In the discharge of the combustor, a movable contraction (52-mm i.d.) was installed. To simulate practical hardware, no wall cooling air was provided.

A research air blast atomizer provided by Parker Hannifin atomized the Jet-A fuel at a nominal 65-deg spray angle. Swirl vanes in the nozzle produced a clockwise swirling flow. Laser diffraction (LD) and phase Doppler interferometry (PDI) measurements confirmed that this nozzle produced a 38-μ Sauter mean diameter 15-mm downstream of the nozzle, with little variation in droplet size as air/liquid mass ratio varied from 2.0 to 3.0.

The swirlers were all of the same basic design. Swirl was produced from 12 curved vanes of uniform thickness, brazed to a hub. Two sets of 45- and 60-deg vanes were fabricated. One set provided a clockwise rotating flow. The other set provided a counterclockwise rotating flow. Geometric swirl numbers calculated from a relation given by Beer and Chigier[19] are 0.8 and 1.4 for the 45- and 60-deg swirlers, respectively. Two different inlet domes were used: 1) a 45-deg conical expansion, and 2) a step (90-deg expansion).

The combustor flow facility has been described elsewhere.[15,18,20] Airflows to the swirler and nozzle were metered using choked venturi nozzles. The swirl air passed through a flow straightening section prior to the swirl vanes. Fuel was provided by way of a reservoir tank pressurized by nitrogen. The airflows were seeded with 1-μ alumina particles using a fluidized bed reservoir. To avoid biasing during the velocity measurements, seed was introduced into the airstreams prior to flow regulation to ensure a uniform distribution.

The combustor and inlet flow hardware were mounted on a traversing beam that provided axial positioning of the combustor. The optics and emissions probe were mounted on a table that traversed in the two orthogonal directions in the horizontal plane.

Diagnostics

Emissions Sampling

A hot water-cooled probe was used to extract sample gases at different radial stations in different axial planes in the combustor. The probe was aligned prior to each test using the laser beam crossing from the laser anemometry system. Accuracy of positioning is estimated to be ± 0.5 mm. The cooling water was supplied to the probe at 90°C to minimize condensation of unburned hydrocarbons (UHC) and deposition of soot by means of thermophoresis.

The sample lines were heated with heat tape to minimize condensation of UHC.[20] The bypass loop passed the gas samples directly into the exhaust emissions analyzer, Horiba model MEXA-554GE, where they were measured for volume percents of CO, CO_2, UHC (as *n*-hexane equivalent), and O_2. The "catalyst" loop oxidized any UHC and CO to CO_2. The gas then passed through a water dropout to provide a dry sample to the analyzer. The instrument was zeroed and calibrated prior to each experimental period. The recalibrations rarely exceeded 5% of the calibrated value.

Table 1 Variable ranges and fixed conditions

Variable	Range
A/L_N	2.0–4.0
V_{ref}, ms	3.75–5.0
S_n	0.8–1.4
θ_D, deg	45–90
L_D, mm	160–240
Air preheat temperature, K	298
Chamber pressure, atm	1
Equivalence ratio	1.5
Fuel	Jet-A
Swirler diameter, mm	34
Dome diameter, mm	80

Laser Anemometry

A 4.0-W Argon-Ion laser provided a multiline beam which was separated into two single line beams at wavelengths of 488.0 and 514.5 nm. The green and blue beams were then split into two beams. Each color had one of the two beams frequency shifted 40 MHz using a Bragg cell. Each set of beams then passed through a focusing lens and formed a probe volume inside the combustor. Axial and azimuthal velocities were measured simultaneously. A set of two TSI model 9162 photomultiplier tubes, one for each component, was used to detect the scattered light produced from the 1.0-μ Al_2O_3 seed particles as they passed through the probe volume. The signals from the PMTs were filtered and processed using two TSI model 1980B frequency counters installed in an IBM PC compatible computer. Software provided on-line cumulative histograms of both velocity components, as well as calculated mean and rms velocities, shear stress values, among other quantities.

Test Matrix

Based on literature studies and experimental flexibility, five parameters were identified to study to characterize dome mixing effectiveness: 1) atomizer air/liquid ratio (A/L_N), 2) dome reference velocity (V_{ref}), 3) swirl number (S_n), 4) dome expansion angle (θ_D), and 5) dome length (L_D).[20] Dome length is defined as the axial distance from the atomizer to the convergent section in the rich zone as illustrated in Fig. 1. The ranges of these variables that were experimentally investigated, as well as the fixed levels of the other variables, are summarized in Table 1.

The dome characterization approach followed four steps: 1) stability limits were identified; 2) mixing performance was determined for several conditions and correlated using a second-order polynomial; 3) mixing performance was optimized using the above correlation; and 4) the optimized conditions were studied to both verify optimum performance and characterize velocity fields at the optimum conditions.

In order to correlate the mixing performance with the five independent variables, a mixing effectiveness index (MEI) was used which combined information about the uniformity of mixing with the extent of reaction as shown in Eq. (1):

$$\mathrm{MEI} = \sqrt{\frac{1}{A}\left[\sum_{i=1}^{n} a_i (C_i - C_{\mathrm{equil}})^2\right]} \qquad (1)$$

where

A = $(\Sigma\, a_i)$, cross-sectional area
C_i = measured concentration
C_{equil} = equilibrium concentration

The MEI is defined as the area weighted standard deviation of gas species about the equilibrium gas composition predicted using the NASA chemical equilibrium code.[21] In this study, the MEI was based on point measurements of carbon monoxide (CO), carbon dioxide (CO_2), oxygen (O_2), and unburned hydrocarbons (UHC) that were obtained using an extractive probe across a fixed axial plane.

Results and Discussion

Stability Evaluation

The dome was operated over the entire range of each independent variable of Table 1 to establish the stability and measurability of each condition. Stability was assessed qualitatively by observation. Conditions were deemed "unstable" if operation proved excessively loud (an indication of high-amplitude pressure fluctuations), if the reaction could not be maintained (i.e., blowout occurred), or if the stability was time dependent. All other conditions were noted as "stable" conditions. Using these criteria, the stability of the combustor was graphed over its operational space. The results are shown in Fig. 2 for variations in reference velocity, swirl direction, nozzle air/liquid ratio and dome expansion angle.

Figures 2a and 2b display the envelope of stability for the 90-deg dome cases. Figures 2c and 2d display the 45-deg dome cases. The variable combinations that occur inside of a gray box correspond to unstable operating conditions. For the variable ranges considered, the coswirling case (clockwise rotating swirlers and clockwise rotating nozzle flow) had a larger number of independent variable combinations that resulted in unstable operation for both the 45- and 90-deg dome expansion angles. This is due in part to excessive fuel transport to the combustor walls. In such cases, initial instabilities were reduced or eliminated as the combustor wall was heated to steady-state conditions.

Because of the relatively poor limits of stable operation when using the coswirling configuration, the experimental investigation focused on the counterswirling experiments.

Mixing Uniformity

A 16-point, two-level fractional factorial test matrix was followed to determine the combined effects of atomizer air/liquid ratio, dome reference velocity, swirl number, dome expansion angle, and dome length on the MEI. Equilibrium calculations were performed for the conditions listed in Table 1 to assess the extent of reaction for each case considered. The equilibrium gas composition was predicted to be 12.0% CO, 5.7% CO_2, 5.4% H_2, 11.4% H_2O, 0.0% O_2, and the balance principally N_2 with small amounts of Ar and NO. The equilibrium calculations were computed using the NASA equilibrium code.[21]

Two radial profiles of CO, CO_2, and O_2 (on moisture-free bases), measured at the exit plane of the dome, are presented in Fig. 3. These profiles are representative of the range of profiles measured in the 16-point test matrix described above.

Figure 3a presents a "nearly uniform" mixture case (A/L_N = 4.0, V_{ref} = 5.0 m/s, θ_D = 45 deg, L_D = 240 mm, S_n = 1.4). Deviation from complete uniformity is evidenced both at the wall and at the centerline. The higher levels of O_2 and CO relative to lower amount of CO_2 near the centerline suggest that the reaction has not gone to completion. For this case, the oxygen concentration is low and approaching the equilibrium value near the combustor wall. However, the CO concentration is higher than the equilibrium value throughout the entire radial profile. It is evident that this case is approaching, but does not yet represent, optimum mixing. In Fig. 3a, the deviations from equilibrium concentration and radial composition uniformity are representative of some of the better cases that were observed.

In Fig. 3b (A/L_N = 2.0, V_{ref} = 5.0 m/s, θ_D = 45 deg, L_D = 160 mm, S_n = 1.4), the increased variations in emissions across the combustor radius indicate nonuniform fuel-air mixing. As in Fig. 3a, evidence of incomplete reaction occurs along the centerline and near the wall. For this case, a zone of intense reaction is centered around the −24-mm measurement location. In addition to the measurements shown, a core of UHC was detected along the combustor centerline.[20] In this case, not only is the mixture uniformity poor, the extent of reaction is poor as well.

Mixing Effectiveness

The composition profiles for each of the 16 cases ranged in their degree of uniformity and extent of reaction between Figs. 3a and 3b. For each case a MEI value was computed using Eq. (1). The MEI values were then used to create the

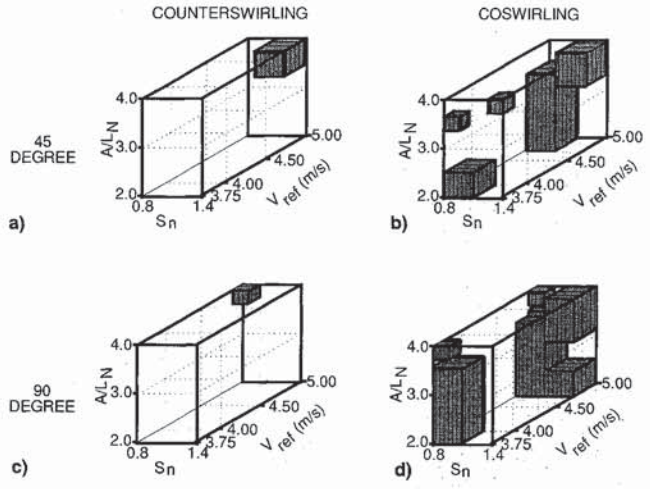

Fig. 2 Stability envelope for a) and b) the 90-deg and c) and d) the 45-deg dome expansion angles. Gray volume = unstable region, white volume = stable region.

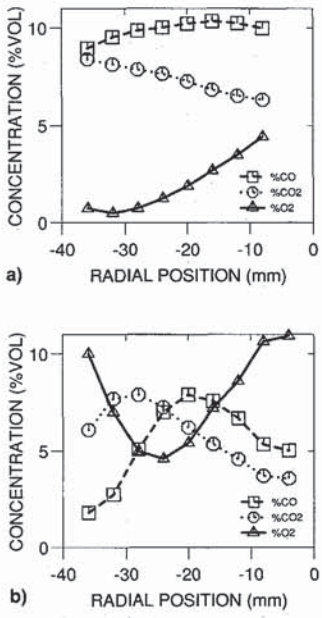

Fig. 3 Representative CO, CO_2, and O_2 radial exit plane profiles in the staged combustor rich zone: a) near uniform and b) nonuniform.

second-order interpolation polynomial shown in Eq. (2). The correlation coefficient for this equation was calculated to be 0.999, and was found to fit the MEI data with no more than a 4% residual in the worst case[20]

$$\begin{aligned}\text{MEI} = {} & C_1 \times A/F_N + C_2 \times \theta_D + C_3 \times V_{\text{ref}} + C_4 \times S_n \\ & + C_5 \times A/F_N \times L_D + C_6 \times A/F_N \times \theta_D + C_7 \times A/F_N \times V_{\text{ref}} \\ & + C_8 \times L_D \times \theta_D + C_9 \times L_D \times V_{\text{ref}} + C_{10} \times L_D \times S_n \\ & + C_{11} \times \theta_D \times S_n \end{aligned} \quad (2)$$

where

$C_1 = 1.293786$
$C_2 = 0.054691$
$C_3 = -0.535394$
$C_4 = 1.882567$
$C_5 = -0.004133$
$C_6 = -0.008116$
$C_7 = -0.069249$
$C_8 = -0.000048$
$C_9 = 0.002836$
$C_{10} = -0.005501$
$C_{11} = -0.015362$

Figures 4a and 4b are plots generated from Eq. (2) for the 45- and 90-deg dome cases, respectively. In these figures, the MEI values are plotted as contours over the ranges of nozzle air/fuel ratio and reference velocities shown. Variable combinations that minimize the MEI value are optimum.

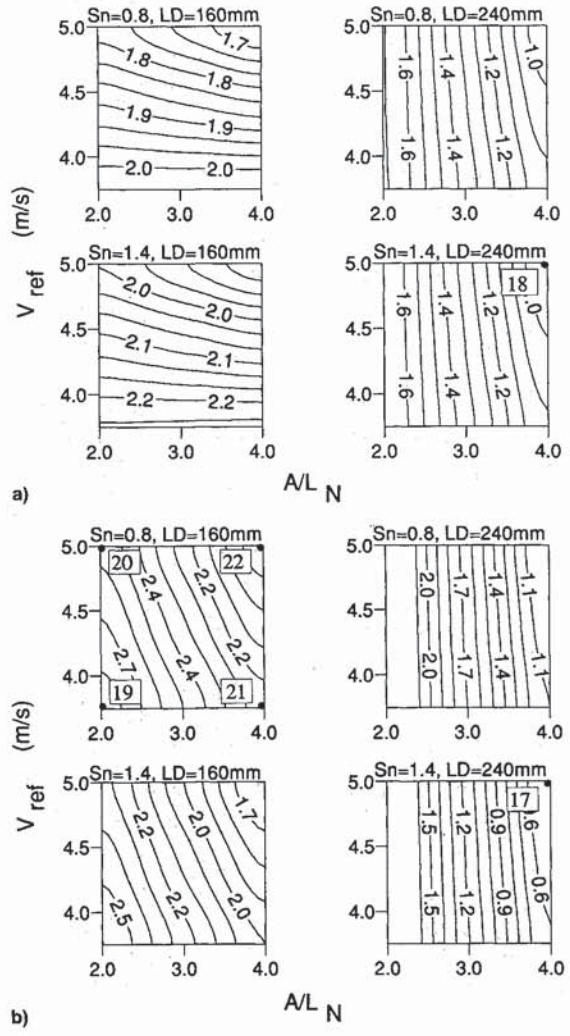

Fig. 4 Mixing effectiveness index (MEI) for a) 45-deg dome and b) 90-deg dome for varying levels of air/fuel ratio, reference velocity, swirl number, dome length, and dome expansion angle.

Figures 4a and 4b illustrate the complex behavior of this combustor dome with changes in dome design and operating parameters. The dome mixing performance can be correlated with the formation and strength of the large scale structures that promote mixing. This is especially evident in comparing the 160-mm dome results to the 240-mm dome results. For the 160-mm dome, the nozzle air/fuel ratio influenced the magnitude of the MEI for the 90-deg dome expansion angle (see Fig. 4b) but was relatively insignificant for the 45-deg dome expansion angle cases (see Fig. 4a). In the 90-deg case, as the nozzle air/fuel ratio increased, the effective spray angle decreased, and the strength of the bluff body recirculation zone in the corner of the dome increased which resulted in better mixing. The 45-deg dome expansion precluded the formation of corner bluff body recirculation regions.

It is interesting to note that the 160-mm dome with a reference velocity of 3.75 m/s has a nominal residence time close to the 240-mm dome with a reference velocity of 5.0 m/s. In spite of this similarity, the performance was markedly different for the two cases. This result indicates that the shorter dome length significantly suppressed the formation and strength of the large scale fluid mechanical structures (such as the recirculation zones) that are required for effective mixing. In the 240-mm dome, where the large scale structures were not suppressed by the downstream restriction, the dominate controlling feature became the nozzle air/fuel ratio. In this case, as the nozzle air/fuel ratio increased, the shrinking effective spray angle matched better with the shear layer of the recirculation zone which, in turn, resulted in better mixing and reaction. This is especially true as the swirl strength increased as evidenced by an increase in swirl number from 0.8 to 1.4.

Both Figs. 4a and 4b suggest that optimum mixing effectiveness occurs at the higher nozzle air/fuel ratios, higher dome reference velocities, higher swirl numbers, and longer dome lengths. In addition, the 90-deg dome expansion angle has a better MEI optimum value compared to the 45-deg dome.

Unlike the improved mixing performance noted by Charles,[16] the 45-deg dome expansion of this study provided mildly degraded performance compared to the 90-deg step expansion.

Large-Scale Structures and Mixing

In order to better understand how mixing quality relates to large scale structures in the flowfield, the axial and tangential velocity profiles were measured for select cases. Figures 5a and 5b present the mean axial (U) and tangential (W) velocities measured at the conditions noted as point 18 and point 17 of Figs. 4a and 4b, respectively. In these figures, many flow features can be identified that are a result of a balance between different competing forces in the flowfield.

In both the 90- and 45-deg dome expansion cases, a strong off-axis recirculation zone is evident. In the 90-deg case, this recirculation zone is strongest near the nozzle. In the 45-deg case, it is strongest at the 40-mm position. In both cases, material near the combustor wall is brought towards the outer radius of the annular swirler. The suppression of the recirculation zone by the 45-deg step expansion is evident. Unlike the 90-deg case, the 45-deg case also features an on-axis recirculation zone at the 20-mm axial station.

The 45-deg expansion also markedly effects the tangential velocity near the nozzle by effectively eliminating the counterswirling motion of the annular swirler. This in turn produces an effective spray angle of 65 deg, compared to 45 deg for the 90-deg expansion case. The nozzle is designed to have a nominal 65-deg spray angle. Beyond the 40-mm station both cases have similar features. At the 120-mm axial station, the azimuthal velocities are all nearly zero, and the trend is quite

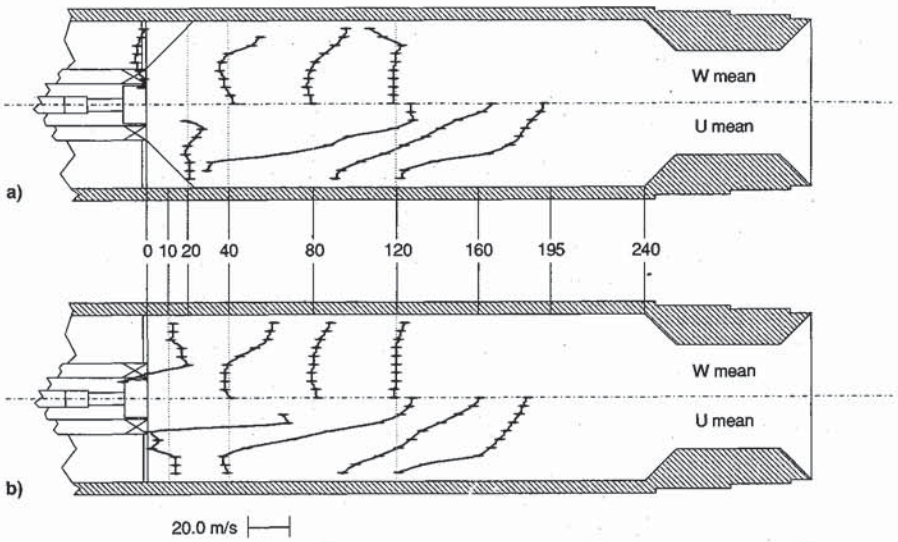

Fig. 5 Mean axial and azimuthal velocity profiles for two near-optimum counterswirling mixing configurations for a) 45-deg dome (noted as case 18 on Fig. 4a) and b) 90-deg dome (noted as case 17 on Fig. 4b).

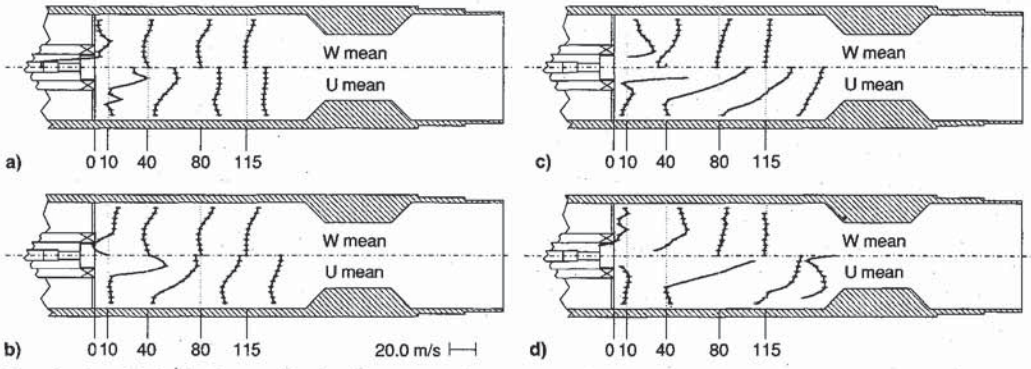

Fig. 6 Mean axial and azimuthal velocity profiles for four nonoptimum counterswirling air and fuel mixing configurations: a) $A/L_N = 2$, $V_{ref} = 3.75$ (m/s) (noted as case 19 on Fig. 4b); b) $A/L_N = 2$, $V_{ref} = 5.00$ (m/s) (noted as case 20 on Fig. 4b); c) $A/L_N = 4$, $V_{ref} = 3.75$ (m/s) (noted as case 21 on Fig. 4b); and d) $A/L_N = 4$, $V_{ref} = 5.00$ (m/s) (noted as case 22 on Fig. 4b).

flat. Consequently, the swirling component of the flow is not being carried beyond the combustor dome.

Effect of Dome Length on Mixing

The negative impact of the 160-mm dome length on flow structures that was discussed above, is evident in the four cases presented in Figs. 6a–d. These cases correspond to the points noted as 19, 20, 21, and 22 in Fig. 4. As in Fig. 5, the U and W velocities are shown.

In addition to being shorter, the annular swirl number is reduced from 1.4 to 0.8, compared to the cases shown in Fig. 5. This results in a much narrower effective spray angle (23 deg) and a very weak off-axis recirculation zone for case 22 (Fig. 6d). The narrow spray angle and the short dome length contribute to the skewed axial velocity profile at the 115-mm axial station. At a nozzle air/fuel ratio of 4, roughly 40% of the total air supplied to the dome passes through the nozzle.

When the reference velocity of case 22 is decreased to 3.75 m/s (see case 21 shown in Fig. 6c), the effective spray angle broadens to 34 deg. This results in the initial reaction zone occurring closer to the nozzle as evidenced by the high velocities near the centerline at the 10-mm station. At this condition the off-axis recirculation zone is still weak and largely ineffective in promoting effective mixing.

Figures 6a and 6b complete the picture. At the nozzle air/fuel ratio of 2, roughly 20% of the total dome air passes through the nozzle. This results in an effective spray angle of 63 deg for both cases 19 and 20 shown in Figs. 6a and 6b, respectively. In these cases, the fuel injection is strongly mismatched with the fluid structures. The annular swirler does not impart enough momentum to create a recirculating flow. Consequently, the mixing is poor and the bulk of the chemical reactions must occur downstream of the dome.

As concluded from Fig. 4, the velocity plots shown in Figs. 5 and 6 confirm the strong sensitivity of the dome region mixing performance to small changes in the dome configuration and operation. The best performing dome configuration featured high levels of turbulence intensity in the near nozzle region. A better understanding of the competing forces will allow combustor design features to be better married to operational constraints.

Summary and Conclusions

An experimental research program was undertaken to study the process of fuel-air mixing within the dome region of a staged gas turbine combustor. The goal of this research was to identify design and operational characteristics that give rise to rapid and complete fuel-air mixing in the dome region and to provide the air addition stage with a uniformly distributed and reacted mixture of product gases.

The conclusions for this study are as follows:

1) Optimum mixing requires balancing several competing forces that arise from both design and operational constraints. The response of mixing effectiveness to changes in any single

variable cannot be considered independently of the other variables.

2) The effects of variation in reference velocity, nozzle-air-to-fuel ratio, swirl strength, inlet geometry, and dome length on fuel-air-mixing are quite complex. In those cases where the nominal dome residence time was the same for different dome lengths, the resulting mixing performance was much different, indicating that the formation and strength of the large scale fluid mechanical structures were affected.

3) Acceptable fuel-air mixing characteristics are obtainable within the operational ranges and with the hardware designs investigated.

4) In the counterswirling nozzle-swirler configuration, simultaneous increases of nozzle air-to-fuel ratio, reference velocity, swirl number and dome length, in general, lead to improved mixing effectiveness.

5) For the hardware studied, coswirling flows greatly reduce stability envelopes compared to their counterswirling analogs.

6) The optimum mixing counterswirling fuel and airstream configuration featured a strong torroidal recirculation zone, an effective spray angle of 45 deg, and azimuthal velocities that have decayed to zero inside of two duct diameters.

Acknowledgment

This work was conducted under funding provided by NASA Lewis Research Center (Grant NAG3-1124) with R. R. Tacina serving as contract monitor.

References

[1]Owen, F. K., Spadaccini, L. J., and Bowman, C. T., "Pollutant Formation and Energy Release in Confined Turbulent Diffusion Flames," *Sixteenth Symposium (International) on Combustion*, The Combustion Inst., Pittsburgh, PA, 1977, pp. 105–117.

[2]Ahmad, N. T., Andrews, G. E., Kowkabi, M., and Sharif, S. F., "Centrifugal Mixing Forces in Enclosed Swirl Flames," *Twentieth Symposium (International) on Combustion*, The Combustion Inst., Pittsburgh, PA, 1985, pp. 259–267.

[3]Alkabie, H. S., and Andrews, G. E., "Ultra-Low NO_x Emissions for Gas and Liquid Fuels Using Radial Swirlers," ASME Paper 89-GT-322, June 1989.

[4]Alkabie, H. S., and Andrews, G. E., "Radial Swirlers with Peripheral Fuel Injection for Ultra-Low NO_x Emissions," American Society of Mechanical Engineers Paper 90-GT-102, June 1990.

[5]Semerjian, H. G., Ball, I. C., and Vranos, A., "Pollutant Emissions from 'Partially' Mixed Turbulent Flames," *Seventeenth Symposium (International) on Combustion*, The Combustion Inst., Pittsburgh, PA, 1979, pp. 697–687.

[6]Rink, K. K., and Lefebvre, A. H., "The Influences of Fuel Composition and Spray Characteristics on Nitric Oxide Formation," *Combustion Science and Technology*, Vol. 68, Nos. 1–3, 1989, pp. 1–14.

[7]Brady, R. A., and Samuelsen, G. S., "Visualization of Dome Region Mixing in a Quartz Combustor," American Society of Mechanical Engineers Paper 91-GT-360, June 1991.

[8]Mosier S. A., Pierce, R. M., Smith, C. E., and Hinton, B. S., "Advanced Combustor Systems for Stationary Gas Turbines," U.S. Environmental Protection Agency, Final Report FR 11405, Contract 68-02-2136, Research Triangle Park, NC, March 31, 1980.

[9]Hatch, M. S., Sowa, W. A., Samuelsen, G. S., and Holdeman, J. D., "Jet Mixing Into a Heated Cross Flow in a Cylindrical Duct," NASA TM 105390, Jan. 1992; see also AIAA Paper 92-0773, Jan. 1992.

[10]Fenimore, C. P., "Formation of Nitric Oxide in Premixed Hydrocarbon Flames," *Thirteenth Symposium (International) on Combustion*, The Combustion Inst., Pittsburgh, PA, 1971, pp. 373–380.

[11]Pompei, F., and Heywood, J. B., "The Role of Mixing in Burner-Generated Carbon Monoxide and Nitric Oxide," *Combustion and Flame*, Vol. 19, No. 3, 1972, pp. 407–418.

[12]Shekleton, J. R., "The CIVIC: A Concept in Vortex-Induced Combustion of the Solar Gemini 10kW Gas Turbine," *Journal of Engineering for Power*, Vol. 103, No. 34, 1981, pp. 34–42.

[13]Wood, C. P., and Samuelsen, G. S., "Optical Measurements of Soot Size and Number Density in a Spray-Atomized, Swirl-Stabilized Combustor," *Journal of Engineering for Gas Turbines and Power*, Vol. 107, No. 1, 1985, pp. 38–47.

[14]Katsuki, M., Mizutani, J., and Shibuya, K., "An Experimental Study on the Emission of a Model of Gas Turbine Combustor," *Combustion Science and Technology*, Vol. 17, No. 11, 1977, pp. 11–18.

[15]Cameron, C. D., Brouwer, J., and Samuelsen, G. S., "A Model Gas Turbine Combustor with Wall Jets and Optical Access for Turbulent Mixing, Fuel Effects and Spray Studies," *Twenty-Second Symposium (International) on Combustion*, The Combustion Inst., Pittsburgh, PA, 1988, pp. 465–474.

[16]Charles, R. C., and Samuelsen, G. S., "An Experimental Data Base for Computational Fluid Dynamics of Combustors," *Journal of Engineering for Gas Turbines and Power*, Vol. 11, No. 1, 1989, pp. 11–14.

[17]Charles, R. C., Emdee, J. L., Muzio, L. J., and Samuelsen, G. S., "The Effect of Inlet Conditions on the Performance and Flowfield Structure of a Non-Premixed, Swirl-Stabilized Distributed Reaction," *Twenty-First Symposium (International) on Combustion*, The Combustion Inst., 1986, pp. 1455–1461.

[18]Brouwer, J., Cameron, C. D., and Samuelsen, G. S., "A Parametric Investigation of a Model Gas Turbine Can Combustor," The 24th AIAA/ASME/ASEE Joint Propulsion Conf., AIAA Paper 88-2859, July 1988.

[19]Beer, J. M., and Chigier, N. A., *Combustion Aerodynamics*, Wiley, New York, 1972.

[20]Brady, R. A., Sowa, W. A., and Samuelsen, G. S., "A Study of Dome Region Fuel-Air Mixing in a Model Rich Burn-Quick Mix-Lean Burn Combustor," NASA TM189112, 1991.

[21]Gordon, S., and McBride, B. J., "Computer Program for Calculation of Complex Chemical Equilibrium Compositions, Rocket Performance, Incident and Reflected Shocks, and Chapman-Jouguet Detonations," NASA SP-273, March 1976.